Miniemulsion Copolymerizations of Methyl Methacrylate and Butyl Acrylate in the Presence of Reactive Costabilizer

C. T. Lin,[1] W. Y. Chiu,[2] H. C. Lu,[2] Y. Meliana,[1] C. S. Chern[1]

[1]*Department of Chemical Engineering, National Taiwan University of Science and Technology, Taipei 106, Taiwan*
[2]*Department of Chemical Engineering, National Taiwan University, Taipei 106, Taiwan*

Received 7 December 2008; accepted 23 February 2009
DOI 10.1002/app.30389
Published online 26 October 2009 in Wiley InterScience (www.interscience.wiley.com).

ABSTRACT: The storage stability and free radical polymerizations of miniemulsions comprising methyl methacrylate (MMA), butyl acrylate (BA), and a reactive costabilizer stearyl methacrylate (SMA) were investigated. The Ostwald ripening rate increases with increasing MMA content in the monomer mixture. Both the pseudo-two-component model and empirical equation with one adjustable parameter k adequately predicted the Ostwald ripening rate data. For the empirical model, the least-squares best fit technique gave a value of k equal to 677.5 and values of Ostwald ripening rate and water solubility equal to $(8.8 \pm 0.2) \times 10^{-21}$ cm^3/s and 1.8×10^{-9} cm^3/cm^3 for SMA, respectively. These two models were combined to impart some physical insight to the parameter k. The kinetic studies showed that the polymerization rate increased with increasing MMA content. This is closely related to the nature of the constituent monomers MMA and BA and the particle nucleation mechanisms. The reactive costabilizer SMA is not hydrophobic enough to completely eliminate the Ostwald ripening effect, thereby increasing the probability of polymer reactions in the continuous aqueous phase. Thus, in addition to monomer droplet nucleation, particle nuclei can be generated in the aqueous phase via homogeneous nucleation. The extent of homogeneous nucleation increased with increasing MMA content and, as a result, the number of reaction loci available for the major polymerization to take place followed the same trend. © 2009 Wiley Periodicals, Inc. J Appl Polym Sci 115: 2786–2793, 2010

Key words: miniemulsion polymerization; three-component disperse phase systems; Ostwald ripening; kinetics; particle nucleation

INTRODUCTION

Monomer miniemulsions are thermodynamically unstable, as evidenced by the gradually increased monomer droplet size upon aging. The solubility of monomer in the continuous aqueous phase increases exponentially with decreasing monomer droplet diameter according to the following equation originally proposed by Kelvin[1]:

$$C_m(d_d) = C_m(\infty) \exp[4\sigma V_m/(RTd_d)] \quad (1)$$

where $C_m(d_d)$ and $C_m(\infty)$ are the solubilities for the monomer droplets with a diameter of d_d and the bulk monomer in water, respectively, σ the droplet-water interfacial tension, V_m the molar volume of monomer in the droplets, R the gas constant, and T the absolute temperature. Thus, larger droplets tend to grow in size at the expense of smaller ones and, ultimately, such a diffusional degradation process will destabilize miniemulsion products (termed the Ostwald ripening effect).

Incorporation of an extremely hydrophobic, low-molecular weight compound (costabilizer) can effectively retard the diffusion of monomer molecules from small droplets to large ones due to the osmotic pressure effect, thereby leading to more stable miniemulsions.[1,2] On the basis of the extended Lifshitz-Slezov-Wagner (LSW) theory, the rate of Ostwald ripening (R_O) for the costabilizer-containing miniemulsions can be calculated by the following equation[1]:

$$R_O = d(d_d^3)/dt = 64\sigma D_c V_m C_c(\infty)/(9RTv_c) \quad (2)$$

where D_c is the molecular diffusivity of costabilizer in water, $C_c(\infty)$ the solubility of the bulk costabilizer in water, and v_c the volume fraction of costabilizer in the monomer droplets. eq. (2) predicts that lowering the oil–water interfacial tension, decreasing the solubility of the bulk costabilizer in water, and increasing the level of costabilizer within the monomer droplets greatly enhance the stability of miniemulsions against the diffusional degradation. Neglecting the effects of V_m and σ, the following Kabalnov equation can reasonably predict the rate of Ostwald ripening for monomer miniemulsions in the presence of costabilizer[3]:

$$1/R_O = (v_m/R_{O,m}) + (v_c/R_{O,c}) \quad (3)$$

where v_m is the volume fraction of monomer in the monomer droplets and $R_{O,m}$ and $R_{O,c}$ represent the

Correspondence to: C. S. Chern (cschern@mail.ntust.edu.tw).

rates of Ostwald ripening for the single-component monomer emulsion and costabilizer emulsion, respectively. The rate of Ostwald ripening is primarily controlled by the hydrophobicity and amount of costabilizer present in the monomer droplets, provided that $R_{O,c}$ is much smaller than $R_{O,m}$. It is noteworthy that a miniemulsion system initially with a broader droplet size distribution exhibits a faster Ostwald ripening rate.[3] The initial droplet size distribution is dependent on the miniemulsion compositions and the homogenization equipments and processes.

Chern and coworkers[4–7] used stearyl methacrylate (SMA) or lauryl methacrylate (LMA) as reactive costabilizers to stabilize styrene miniemulsion polymerizations. Just like conventional costabilizers (e.g., hexadecane), long-chain alkyl methacrylates, act as costabilizers in stabilizing the homogenized submicron monomer droplets. Furthermore, the methacrylate group of polymerizable costabilizers can be chemically incorporated into latex particles in the subsequent free radical polymerization and thereby reduce the level of volatile organic compounds (VOC). Emulsified monomer droplets (~1–10 μm in diameter, 10^{12}–10^{14} dm^{-3} in number density) are generally not considered to contribute to the particle nucleation process to any appreciable extent in conventional emulsion polymerization. However, homogenized submicron monomer droplets may become the predominant particle nucleation loci (monomer droplet nucleation).[8,9] These tiny monomer droplets have an extremely large total droplet surface area and, therefore, they may compete effectively with micellar nucleation[10–12] and homogeneous nucleation[13–15] for the oligomeric radicals generated in the continuous aqueous phase. Chern and coworkers[16–19] used a water-insoluble dye as the molecular probe for the particle nucleation loci in styrene (ST) miniemulsion polymerizations stabilized by a surfactant concentration lower than its micelle concentration. These studies illustrate that formation of particle nuclei in the aqueous phase cannot be completely eliminated even for the miniemulsion polymerizations of the relatively hydrophobic ST. Thus, a competitive particle nucleation mechanism involving both monomer droplet nucleation and homogeneous nucleation was proposed.

In our recent work,[20] the extended Kabalnov equation shown below failed to predict the Ostwald ripening rate for the three-component disperse phase miniemulsions comprising ST, methyl methacrylate (MMA) and SMA.

$$1/R_O = (v_1/R_{O,1}) + (v_2/R_{O,2}) + (v_3/R_{O,3}) \quad (4)$$

where the subscripts 1, 2 and 3 represent ST, MMA, and SMA, respectively. It is noteworthy that, although the above statement about eq. (4) is still valid, a mistake was made in the calculation of R_O (i.e., the weight fractions of the components were used instead of the volume fractions). The following empirical model was then proposed to adequately predict the Ostwald ripening rate data over a wide range of monomer compositions

$$1/R_O = k[(v_1/R_{O,1}) + (v_2/R_{O,2})] + (v_3/R_{O,3}) \quad (5)$$

where k is an adjustable parameter. Nevertheless, no physical meanings behind this parameter were given. The objective of this study was to examine the general validity of this empirical model [eq. (5)] in describing other three-component disperse phase miniemulsion systems comprising acrylic monomers, MMA, butyl acrylate (BA) and SMA. Another major thrust of this project was to gain a fundamental understanding insight into the parameter k in eq. (5). Free radical polymerizations of the resultant monomer miniemulsions were then carried out to investigate the effect of Ostwald ripening on the relevant polymerization kinetics and mechanisms.

EXPERIMENTAL

Materials

The chemicals used include MMA and BA (Kaohsiung Monomer), SMA (Aldrich), sodium lauryl sulfate (SLS, J.T. Baker, 99%), sodium persulfate (SPS, Riedel de Haen), sodium bicarbonate (Riedel de Haen) as buffer, hydroquinone (HQ, Nacalai Tesque) as inhibitor and a water-insoluble dye (Blue 70, Shenq-Fong Fine Chemical, China). Other reagents used include methanol, ethanol, acetone, *n*-methyl pyrolidone (NMP), d-chloroform, pure nitrogen gas, magnesium sulfate anhydrous (Yakuri Chemicals), and deionized water (Barnsted, Nanopure Ultrapure Water System, specific conductance < 0.057 μS/cm). SMA was recrystallized in ethanol, and MMA and BA distilled under reduced pressure before use. Other chemicals were used as received.

Preparation and characterization of miniemulsions

The miniemulsion was prepared by dissolving SLS in water and SMA in the mixture of MMA and BA, respectively. The oily and aqueous solutions were mixed using a mechanical agitator at 400 rpm for 10 min. The resultant emulsion was then homogenized with an ultrasonic homogenizer (Misonic sonicator 3000) for 6 cycles of 5 min in length with 2 min off-time, and the output power set at 60% (30 W). A typical miniemulsion formulation comprises the continuous phase (190 g of water, 2.66 m*M* of sodium bicarbonate and 5 m*M* of SLS), the monomer charge (50 g of monomers (MMA and BA), dye (0.1 wt %

based on total monomer) and 20 m*M* of SMA), and the initiator solution (10 g of water and sodium persulfate (0.3 wt % based on total monomer)). The concentrations of sodium bicarbonate, SLS and SMA are based on total water. The variable chosen for study is the weight ratio of MMA to BA (MMA/BA (w/w) = 0/100, 25/75, 50/50, 75/25, 100/0). For comparison, the two-component disperse phase miniemulsions (MMA/BA = 0/100 and 100/0) were also included in this study.

The average hydrodynamic droplet diameters of miniemulsion samples upon aging were determined by dynamic light scattering (DLS; LPA, Photal LPA-3000/3100). The sample was diluted with water to adjust the number of photons counted per s (cps) to 8000–12000. The dilution water was saturated with SLS and monomers and, consequently, diffusion of SLS and monomers from monomer droplets into the continuous aqueous phase was prohibited.

Synthesis and characterization of miniemulsion polymers

Immediately after homogenization, the resultant miniemulsion was charged into a 500-mL reactor equipped with a four-bladed fan turbine agitator, a thermocouple, and a reflux condenser and then purged with N_2 for 10 min while the temperature was brought to 65°C. The initiator solution was then charged into the reactor to start the polymerization. The reaction temperature was kept constant at 65°C and the agitation speed at 250 rpm. The latex product was filtered through a 40-mesh (0.42 mm) and 200-mesh (0.074 mm) screens in series to collect filterable solids. Scraps adhering to the agitator, thermometer, and reactor wall were also collected. The total solids content and the overall conversion of monomers (X) were determined gravimetrically. The average particle diameters of the final latex products and their corresponding dried polymer particles were measured by DLS and TEM (JEOL, TEM-1200 EXII), respectively. The zeta potential (ζ) of latex particles was determined by Zetamaster (Malvern).

The latex samples taken during polymerization were first coagulated by the addition of magnesium sulfate. Unincorporated dye, residue initiator and monomers, surfactant, inhibitor, and magnesium sulfate were washed away using excessive methanol by mixing in a supersonic cleaner. Precipitated polymer particles were then rinsed twice with an excess of water. Approximately 0.1 g of dried polymer was dissolved in 20 mL of NMP for the determination of dye content by the ultraviolet (UV) absorbance method (Shimadzu, UV-160A). The extinction coefficient obtained from the calibration curve of the characteristic UV absorbance at 675 nm versus the dye concentration (0–1.4 $\times$ 10^{-5} g/mL) data were 8.6633 $\times$ 10^4 mL/cm g. The reported weight percentage of dye ultimately incorporated into latex particles (P_{dye}) represents the average of six measurements. The copolymer composition data obtained from ^{1}H-NMR (Varian Gemin 2000, 500 MHz) were used to calculate the individual monomer conversions. The glass transition temperature of copolymer was measured by DSC (TA 2000).

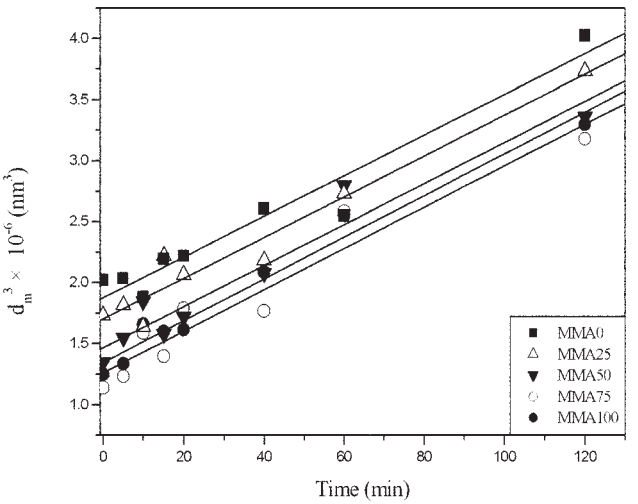

Figure 1 Average monomer droplet diameter as a function of time for miniemulsion samples with varying monomer compositions stabilized by SLS and SMA upon aging at 30°C. MMA/BA (w/w) = (■) 0/100 (R^2 = 0.9427); (□) 25/75 (R^2 = 0.9499); (▼) 50/50 (R^2 = 0.9384); (○) 75/25 (R^2 = 0.9319); (●) 100/0 (R^2 = 0.9734). R^2 represents the coefficient of determination of the least-squares best-fitted straight line shown in this plot.

RESULTS AND DISCUSSION

Miniemulsion stability

The monomer droplet growth mechanism is mainly controlled by Ostwald ripening and osmotic pressure effects. In this study, miniemulsion degraded by coalescence, which requires close contact between two droplets, is assumed insignificant due to the presence of SLS. According to the LSW theory,[3] the Ostwald ripening rate (R_O) for the miniemulsion systems upon aging at 30°C was obtained from the least-squares best fitted d_m^3-vs.-time straight line, as shown in Figure 1. The relatively low values of the coefficient of determination (R^2) reflect the rather scattered miniemulsion stability data based on the dynamic light scattering technique. Consistent with eq. (2), the Ostwald ripening rate increases with increasing weight fraction of MMA (Table I), indicating that the water solubilities of the constituents have a significant effect on the rate of ripening (water solubility in decreasing order: MMA > BA

TABLE I
Some Kinetic Parameters Obtained from Miniemulsion Copolymerizations of MMA and BA in Presence of Reactive Costabilizer SMA at 65°C

MMA/BA (w/w)	0/100	25/75	50/50	75/25	100/0
$R_O \times 10^{19}$ (cm^3/s)	2.78	2.79	2.81	2.83	2.85
$d_{m,i}$ (nm)[a]	111.6	114.2	112.1	104.4	107.5
$d_{p,f}$ (nm)[b]	89.6/88.2	88.6/85.6	85.0/83.2	84.4/81.3	76.6/74.9
$N_{m,i} \times 10^{-17}$ (1/L)[c]	3.8	3.5	3.7	4.5	4.1
$N_{p,f} \times 10^{-17}$ (1/L)[d]	6.2/6.6	6.2/7.8	6.9/10.1	6.9/17.8	8.9/26.4
$N_{p,f}/N_{m,i}$[e]	1.6/1.7	1.8/2.2	1.9/2.7	1.5/4.0	2.2/6.4
$P_{dye,f}$ (%)[f]	88.1	81.2	72.3	52.5	50.3
Total scraps (%)	0.01	0.02	0.03	0.02	0.03

[a] Initial monomer droplet diameter (DLS).
[b] Final latex particle diameter (DLS/TEM).
[c] Initial number of monomer droplets (DLS).
[d] Final number of latex particles (DLS/TEM).
[e] DLS for both $N_{m,i}$ and $N_{p,f}$/DLS for $N_{m,i}$ and TEM for $N_{p,f}$.
[f] Final dye content.
The subscript i represents initial, and f represents final.

>> SMA). Figure 2 shows that the extended Kabalnov equation is incapable of predicting the Ostwald ripening rate data. The mechanism responsible for the failure of this model is not clear at this point of time, but the effects of the molar volume and the droplet-water interfacial tension associated with the very complicated three-component disperse phase systems may contribute to this result.

In our previous work,[20] a pseudo-two-component model that treated the mixture of ST and MMA as component I and SMA as component II in Kabalnov equation was developed to describe the Ostwald ripening behavior of the three-component disperse phase systems comprising ST, MMA, and SMA. However, the model predictions deviated significantly from the experimental data. One alternative of the pseudo-two-component approach (see eq. (6)) proposed in this study treats the mixture of MMA and SMA (MMA/BA/SMA = 100/0/3) as component I (i.e., the run MMA100 in this work) and that of BA and SMA (MMA/BA/SMA = 0/100/3) as component II (i.e., MMA0). Mixing the two components I and II at different ratios (I/II (w/w) = 25/75, 50/50, and 75/25) results in the pseudo-two-component systems chosen for study, designated as MMA25, MMA50, and MMA75, respectively. It should be noted that the SMA content was kept constant (20 m*M* based on total water) in this series experiments.

$$1/R_O = (v_I/R_{O,I}) + (v_{II}/R_{O,II}) \quad (6)$$

$$v_I = (V_1' + V_3')w_I/[(V_1' + V_3')w_I + (V_2'' + V_3'')w_{II}] \quad (7)$$

$$v_{II} = (V_2'' + V_3'')w_{II}/[(V_1' + V_3')w_I + (V_2'' + V_3'')w_{II}] \quad (8)$$

where the numbers 1, 2, and 3 appearing in the subscripts represent MMA, BA and SMA, respectively, $w_I + w_{II} = 1$, v_I and v_{II} are the volume fractions of the component I and II in the pseudo-two-component system, respectively, and $v_I + v_{II} = 1$. V_i' and V_i'' are the volumes of the component i (i = 1, 2, and 3) in the monomer mixture I and II, respectively. The densities used to calculate V_i' and V_i'' are 0.938, 0.894, and 0.864 g/cm^3 for MMA, BA, and SMA, respectively.[21] With the knowledge of the experimental values of $R_{O,I}$ and $R_{O,II}$, the current pseudo-two-component model gives reasonable predictions; the Ostwald ripening rate increases with increasing weight fraction of MMA, as shown in Figure 2. Furthermore, the calculated Ostwald ripening rates are always slightly higher than the experimental data except the two end points.

The general validity of the empirical model [eq. (5)] that was shown successful in describing the

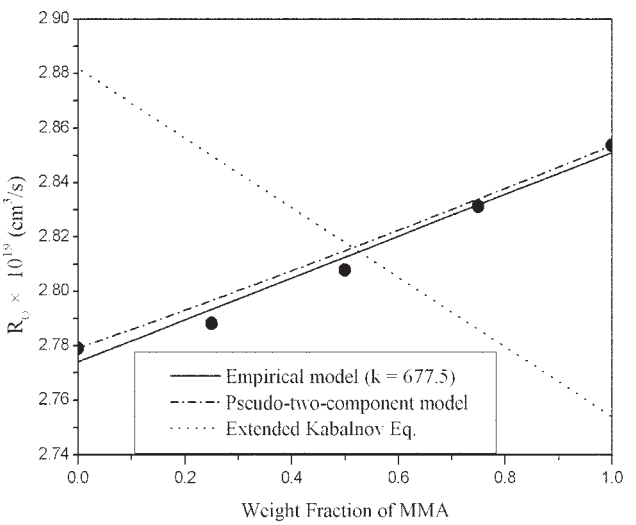

Figure 2 Ostwald ripening rate as a function of MMA weight fraction for miniemulsion samples stabilized by SLS and SMA upon aging at 30°C.

TABLE II
Some Stability Parameters Obtained from Three-Component Disperse Phase Miniemulsions Upon Aging at 30°C or Taken from Literature

Systems	k	$R_{O,3} \times 10^{21}$ (cm^3/s)	Water Solubility of SMA $\times 10^9$ (cm^3/cm^3)	Reference
ST-SMA	–	–	3.23	6
MMA-ST-SMA	555.77	8.77	1.9	20
MMA-BA-SMA	677.50	8.84 ± 0.2	1.8	This work

miniemulsion stability of the three-component disperse phase systems comprising ST, MMA, and SMA[20] was also investigated. Plotting $1/R_O$ vs. $(v_1/R_{O,1}) + (v_2/R_{O,2})$ will result in a straight line with a slope of k and an intercept of $v_3/R_{O,3}$. The Ostwald ripening rate data for the constituent components MMA ($R_{O,1} = 3.97 \times 10^{-14}$ cm^3/s) and BA ($R_{O,2} = 5.77 \times 10^{-15}$ cm^3/s) were obtained from the correlation established in Ref. 21 with the water solubilities of MMA and BA equal to 1.6×10^{-2} and 2.29×10^{-3} cm^3/cm^3, respectively. The least-squares best-fitted technique gave values of k and $R_{O,3}$ equal to 677.5 and $(8.8 \pm 0.2) \times 10^{-21}$ cm^3/s, respectively ($R^2 = 0.9913$, also see the solid line in Fig. 2). It should be noted that an average value of $R_{O,3}$ was reported here because v_3 varied slightly in this series of experiments due to the different densities of MMA and BA. According to Ref. 21 and the best-fitted value of $R_{O,3}$, the water solubility of SMA was then estimated to be 1.8×10^{-9} cm^3/cm^3, which is comparable to the literature data.[6] Some results obtained from this study and the literature data are summarized in Table II. It seems that the k values reflect the overall polarity of constituent components; the larger the k value, the more hydrophilic the constituent components (water solubility: MMA > BA > ST >> SMA). However, more experimental data are required to verify this speculation.

Neglecting the minute difference in the model predictions, the pseudo-two-component and empirical equations can be combined to give an expression containing measurable variables for k:

$$k = \{[(v_I/R_{O,I}) + (v_{II}/R_{O,II})] - (v_3/R_{O,3})\}/[(v_1/R_{O,1}) + (v_2/R_{O,2})] \quad (9)$$

Based on the recipes MMA25, MMA50, and MMA75 and the experimentally determined Ostwald ripening rate data, according to eq. (9), the calculated value of k is 510 ± 10, which is quite close to the least-squares best-fitted value (677.5). It can be shown that eq. (6) is reduced to the extended Kabalnov equation [eq. (4)] and k is equal to 1 if the original Kabalnov equation [eq. (3)] were used to attain $R_{O,I}$ and $R_{O,II}$. However, the extended Kabalnov equation with the least-squares best-fitted value of $R_{O,3}$ is not applicable to the current three-component dispersed phase systems (Fig. 2). Interesting enough, eq. (4) predicts that R_O decreases with increasing MMA content in the monomer mixture. This is most likely due to the very different densities of the constituent components (0.938, 0.894, and 0.864 g/cm^3 for MMA, BA, and SMA, respectively) involved in this series of experiments. As a result, the volume fraction of SMA with the lowest Ostwald ripening rate ($R_{O,3} = (8.8 \pm 0.2) \times 10^{-21}$ cm^3/s) increases from 0.0301 to 0.0315 when the weight ratio of MMA/BA increases from 0/100 to 100/0. This will make the last term ($v_3/R_{O,3}$) on the right hand side of eq. (4) even more important in determining the Ostwald ripening rate for the miniemulsion containing a higher level of MMA. The failure of the extended Kabalnov equation implies that, in addition to the Kabalnov equation itself, another possible explanation for the failure of the extended Kabalnov equation is the presence of coalescence of monomer droplets upon aging. This will lead to the overestimated Ostwald ripening rate and, consequently, the underestimated water solubility of SMA. If this were the case, then the parameter k in eq. (5) might reflect the extent of coalescence of miniemulsion droplets upon aging.

Miniemulsion polymerization

Polymerizations with varying weight ratios of MMA/BA were stabilized by 5 m*M* SDS and 20 m*M* SMA based on the aqueous phase and initiated by

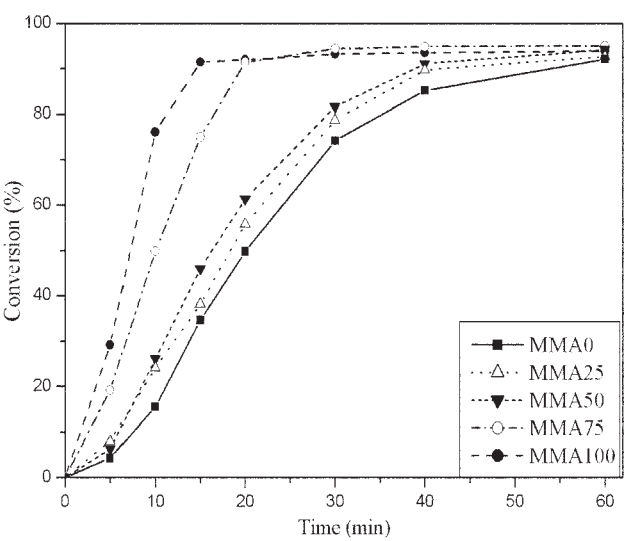

Figure 3 Overall monomer conversion as a function of time for miniemulsion copolymerizations with varying monomer compositions stabilized by SLS and SMA at 65°C. MMA/BA (w/w) = (■) 0/100; (□) 25/75; (▼) 50/50; (○) 75/25; (●) 100/0.

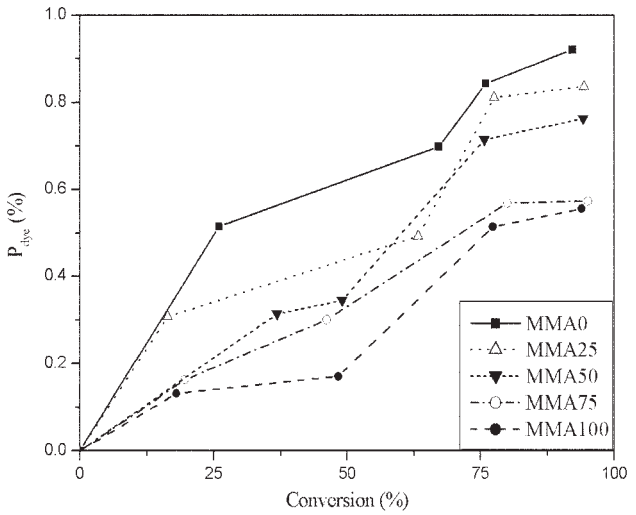

Figure 4 Percentage of dye ultimately incorporated into latex particles as a function of overall conversion for miniemulsion copolymerizations with varying monomer compositions stabilized by SLS and SMA at 65°C. MMA/BA (w/w) = (■) 0/100; (□) 25/75; (▼) 50/50; (○) 75/25; (●) 100/0.

water-soluble initiator SPS (0.3 wt % based on total monomer weight) at 65°C. The average total scraps collected at the end of polymerization are about 0.01–0.03%, indicating satisfactory colloidal stability during polymerization (Table I). Figure 3 shows the overall monomer conversion (X) vs. time profiles. The polymerization rate increases with increasing MMA content in the monomer mixture primarily due to the increased number of reaction loci ($N_{p,f}$) available for polymerization (Table I). $N_{p,f}$ represents the total number of latex particles per unit volume of water at the end of polymerization. Furthermore, the number of monomer droplets initially present in the reaction system ($N_{m,i}$) do not vary very much in the series of experiments (Table I). Thus, in addition to monomer droplet nucleation, more latex particles can be produced in the polymerization system with a higher MMA content as a result of formation of particle nuclei in the continuous aqueous phase (homogeneous nucleation). Besides, the propagation rate constant of MMA is larger than BA ($k_{p,\mathrm{MMA}}$ = 640 L/mol s,[22] $k_{p,\mathrm{BA}}$ = 107 L/mol s[23] at 70°C). Both factors support the observed trend about the polymerization kinetics.

The micellar nucleation mechanism can be ruled out because the SLS concentration is lower than its CMC. Neglecting the coalescence of monomer droplets, a value of $N_{p,f}/N_{m,i}$ equal to unity would imply that monomer droplets per unit volume of water initially present in the polymerization system are all successfully nucleated during polymerization. The fact that all the experimental values of $N_{p,f}/N_{m,i}$, estimated either by DLS or TEM, are greater than one suggests that homogeneous nucleation plays a crucial role in the polymerization kinetics (Table I). Furthermore, the value of $N_{p,f}/N_{m,i}$ increases with increasing MMA content in the monomer mixture (Table I), thereby indicating that the degree of homogeneous nucleation increases with increasing MMA content. It should be noted that the $N_{p,f}/N_{m,i}$ data reported herein and the relevant discussion should be considered qualitative only due to the inherent instrumental limitations.

A significant difference in P_{dye} data was observed for the two polymerizations with MMA/BA = 100/0 and 0/100 (see Table I and Fig. 4), because the water solubility of MMA (159 mM) is one order of magnitude greater than that of BA (16 mM). As would be expected, the miniemulsion polymerization system containing a more hydrophilic monomer mixture promotes the formation of particle nuclei in the continuous aqueous phase, thereby leading to a lower

TABLE III
Overall and Individual Monomer Conversions, Copolymer Compositions and Glass Transition Temperatures for Samples Taken During Miniemulsion Copolymerizations with Varying Compositions at 65°C

Sample ID	X (%)	X_{MMA}[a] (%)	X_{BA}[b] (%)	MMA content[c] (%)	BA content[d] (%)	T_g (°C)
MMA25	16.4	24.9	13.6	37.9	62.1	−9
	63.3	73.3	60	28.9	71.1	−15, 28
	77.6	81.8	76.1	26.4	73.6	−13, 25
	94.3	88.3	96.3	23.4	76.6	−17, 35
MMA50	36.9	45.6	28.2	61.8	38.2	22
	49.1	57.1	41	58.2	41.8	23
	75.8	77.7	73.8	51.3	48.7	24,32, 39
	94.2	90.2	98.2	47.9	52.1	27
MMA75	19.6	22.2	11.9	84.9	15.1	31, 41, 56
	46.2	49.9	35.2	81.0	19.0	37, 50
	80.1	77.9	86.8	72.9	27.1	35, 49
	95.1	91.8	95.4	72.4	27.6	36, 54

[a] Individual conversion of MMA
[b] Individual conversion of BA
[c] MMA content in copolymer
[d] BA content in copolymer

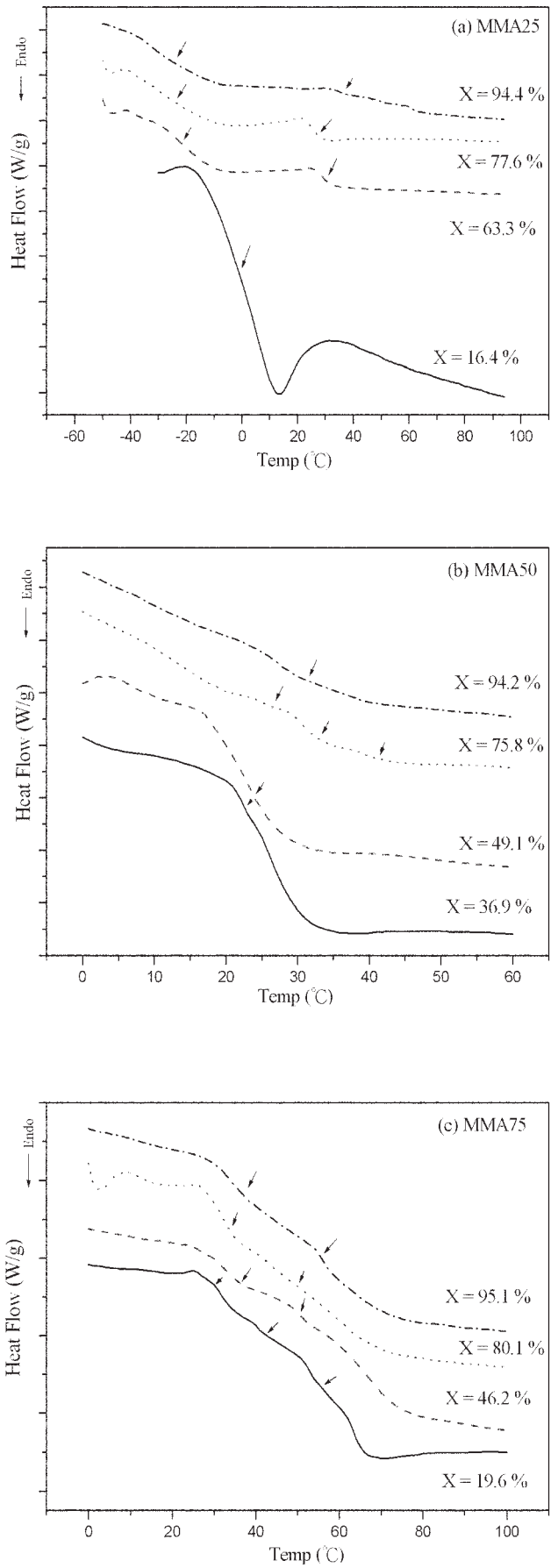

value of P_{dye}. Furthermore, at constant overall monomer conversion, P_{dye} decreases with increasing MMA content, which is consistent with the above $N_{m,i}/N_{p,f}$ data. The smaller the P_{dye} value, the stronger the formation of particle nuclei in water. P_{dye} increases with increasing conversion for all the polymerizations investigated in this work. This indicates that particle nuclei form continuously during the polymerization. Monomer droplet coalescence (if present) results in the desorption of surfactant molecules as a result of the decrease of the total droplet surface area. Thus, the aqueous phase polymer reactions (homogeneous nucleation) are greatly enhanced.

Table III lists the overall and individual monomer conversion data. These results show that the consumption of MMA by free radical polymerization is always faster than BA, which is consistent with the kinetic data shown in Figure 3. This is because MMA has higher propagation rate constant and reactivity ratio compared to BA (r_{MMA}= 2.86, r_{BA}= 0.11[24]). The DSC curves for the resultant copolymers of MMA25, MMA50, and MMA75 at different overall monomer conversions are shown in Figure 5, in which some potential transitions are indicated by the arrow signs and the corresponding glass transition temperature (T_g) data listed in Table III. For reference, the glass transition temperatures of PMMA and PBA are 105°C and −54°C, respectively.[25] Copolymers obtained from solution copolymerizations of MMA and BA only exhibited a single glass transition.[26] However, this is not the case in this series of experiments; very often multi-transitions can be observed in Figure 5. This is attributed to the mixed mode of particle nucleation (i.e., monomer droplet nucleation/homogeneous nucleation). The copolymer composition formed in the particle nuclei originating from homogeneous nucleation could be quite different from those formed in the polymerized monomer droplets.

The zeta potential (ξ) data for the final latex particles as a function of the MMA content in the monomer mixture are shown in Figure 6. The ξ value decreases significantly when the MMA content is increased. This is because a larger population of smaller latex particles via homogeneous nucleation can be achieved in the polymerization system with a higher MMA/BA ratio (see the $N_{p,f}$ and $d_{p,f}$ data in Table I). At constant weight of monomers, the total particle surface area is inversely proportional to the particle size. Thus, at constant surfactant weight, the surface concentration of surfactant decreases with increasing

Figure 5 DSC curves for copolymers obtained at low, medium, and high overall monomer conversions for miniemulsion copolymerizations with varying monomer compositions stabilized by SLS and SMA at 65°C. MMA/BA (w/w) = (a) 25/75; (b) 50/50; (c) 75/25. Some potential transitions are indicated by the arrow signs.

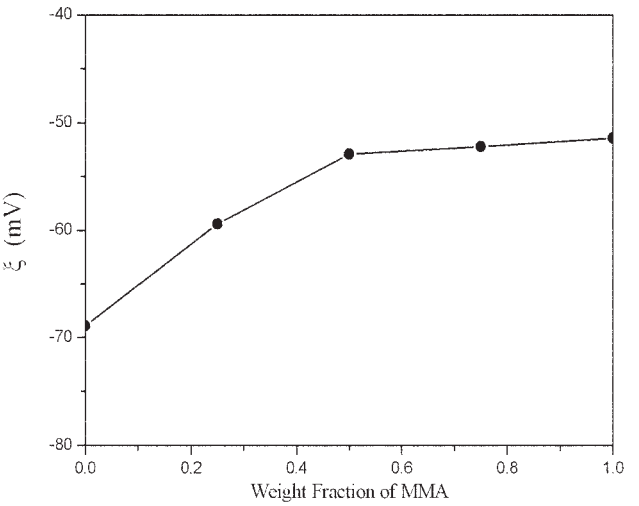

Figure 6 Zeta potential of the final latex particles as a function of MMA weight fraction for miniemulsion copolymerizations stabilized by SLS and SMA at 65°C.

MMA content. Another factor that comes into play is the increased particle surface polarity with MMA content. The higher the particle surface polarity, the smaller the amount of SLS that can be adsorbed on the latex particles. This will then result in a decreased surface charge density (or ζ) with MMA content.

CONCLUSIONS

The storage stability and free radical polymerizations of the three-component disperse phase miniemulsions of different monomer compositions (MMA/BA (w/w) = 0/100, 25/75, 50/50, 75/25, 100/0) in the presence of a reactive costabilizer SMA were investigated. The amount of SMA was kept constant throughout this work. Upon aging at 30°C, the Ostwald ripening rate increases with increasing MMA content in the monomer mixture. Both the pseudo-two-component model and empirical equation with one adjustable parameter k adequately predicted the Ostwald ripening rate data. The key feature of the pseudo-two-component model is to treat the mixture of MMA and SMA (MMA/BA/SMA = 100/0/3) as component I and that of BA and SMA (MMA/BA/SMA = 0/100/3) as component II in Kabalnov equation. Mixing the two components I and II at different ratios then results in the pseudo-two-component systems. Two experimentally determined Ostwald ripening rate data $R_{O,I}$ and $R_{O,II}$ are required to carry out the model predictions. For the empirical model, the least-squares best fit technique gave a value of k equal to 677.5 and values of Ostwald ripening rate and water solubility equal to $(8.8 \pm 0.2) \times 10^{-21}$ cm^3/s and 1.8×10^{-9} cm^3/cm^3 for SMA, respectively. These two models were combined to impart some physical insight to the parameter k. In addition, the empirical equation can be reduced to the extended Kabalnov equation ($k = 1$), which completely failed to describe the Ostwald ripening behavior, if the original Kabalonov equation were used to obtain $R_{O,I}$ and $R_{O,II}$.

The kinetic studies showed that the polymerization rate increased with increasing MMA content. This is closely related to the nature of the constituent monomers MMA and BA (MMA has higher propagation rate constant and reactivity ratio than BA) and the particle nucleation mechanisms. The reactive costabilizer SMA with a water solubility of 1.8×10^{-9} cm^3/cm^3 is not hydrophobic enough to completely eliminate the Ostwald ripening effect, thereby increasing the probability of polymer reactions in the continuous aqueous phase. Thus, in addition to monomer droplet nucleation, particle nuclei can be generated in the aqueous phase via homogeneous nucleation. The extent of homogeneous nucleation increased with increasing MMA content and, as a result, the number of reaction loci available for the major polymerization to take place followed the same trend.

References

1. Kabalnov, A. S.; Shchukin, E. D. Adv Colloid Interface Sci 1992, 38, 69.
2. Higuchi, W. I.; Makarov, J.; Pertzov, A. V.; Shchukin, E. D. J Colloid Interface Sci 1990, 138, 98.
3. Taylor, P. Adv Colloid Interface Sci 1998, 75, 107.
4. Chern, C. S.; Chen, T. J. Colloid Polym Sci 1997, 245, 546.
5. Chern, C. S.; Chen, T. J. Colloid Polym Sci 1997, 245, 1060.
6. Chern, C. S.; Chen, T. J. Colloid Surf A 1998, 138, 65.
7. Chrern, C. S.; Liou, Y. C.; Chen, T. J. Macromol Chem Phys 1998, 199, 1315.
8. Ugelstad, J.; El-Aasser, M. S.; Vanderhoff, J. W. J Polym Sci, Polym Lett ed 1973, 11, 503.
9. Ugelstad, J.; Hamsen, F. K.; Lange, S. Macromol Chem 1974, 175, 507.
10. Harkins, W. D. J Am Chem Soc 1947, 69, 1428.
11. Smith, W. V.; Ewart, R. W. J Chem and Phys 1948, 16, 592.
12. Smith, W. V. J Am Chem Soc 1948, 70, 3695.
13. Roe, C. P. Ind Eng Chem 1968, 60, 20.
14. Fitch, R. M.; Prenosil, M. B.; Sprick, K. J. J Polym Sci 1969, 27, 95.
15. Hansen, F. K.; Ugelstad, J. J Polym Sci, Polym Chem Ed 1978, 16, 1953.
16. Chern, C. S.; Chen, T. J.; Liou, Y. C. Polymer 1998, 39, 3767.
17. Chern, C. S.; Liou, Y. C. Macromol Chem Phys 1998, 199, 2051.
18. Chern, C. S.; Liou, Y. C. Polymer 1999, 40, 3763.
19. Chern, C. S. Principles and Applications of Emulsion Polymerization; Wiley: 2008; pp 137–139.
20. Chern, C. S.; Lim, H.; Cala, N. A. J Appl Polym Sci 2009, 112, 173.
21. Tauer, K. Polymer 2005, 46, 1385.
22. Cameron, G. G.; Kerr, G. P. J Polym Sci, A1 1969, 7, 3067.
23. Delgado, J. J Polym Sci Part A: Polym Chem 1986, 24, 861.
24. Brosse, J. C.; Gauthier, J. M.; Lenain, J. C. Macromol Chem 1983, 184, 505.
25. Satas, D., Ed. Handbook of Pressure-Sensitive Adhesive Technology; Van Nostrand Reinhold, 1982; pp 306.
26. Fernandez-Garcia, M.; Cuervo-Rodriguez, R.; Madruga, E. L. J Polym Sci Part B: Polym Phys 2000, 37, 2512.